

Measurement of the $D^*(2010)^+$ meson width and the $D^*(2010)^+ - D^0$ mass difference

J. P. Lees,¹ V. Poireau,¹ V. Tisserand,¹ E. Grauges,² A. Palano^{ab,3} G. Eigen,⁴ B. Stugu,⁴ D. N. Brown,⁵
L. T. Kerth,⁵ Yu. G. Kolomensky,⁵ M. J. Lee,⁵ G. Lynch,⁵ H. Koch,⁶ T. Schroeder,⁶ C. Hearty,⁷ T. S. Mattison,⁷
J. A. McKenna,⁷ R. Y. So,⁷ A. Khan,⁸ V. E. Blinov^{ac,9} A. R. Buzykaev^{a,9} V. P. Druzhinin^{ab,9} V. B. Golubev^{ab,9}
E. A. Kravchenko^{ab,9} A. P. Onuchin^{ac,9} S. I. Serednyakov^{ab,9} Yu. I. Skovpen^{ab,9} E. P. Solodov^{ab,9}
K. Yu. Todyshev^{ab,9} A. N. Yushkov^{a,9} D. Kirkby,¹⁰ A. J. Lankford,¹⁰ M. Mandelkern,¹⁰ B. Dey,¹¹
J. W. Gary,¹¹ O. Long,¹¹ G. M. Vitug,¹¹ C. Campagnari,¹² M. Franco Sevilla,¹² T. M. Hong,¹² D. Kovalskyi,¹²
J. D. Richman,¹² C. A. West,¹² A. M. Eisner,¹³ W. S. Lockman,¹³ A. J. Martinez,¹³ B. A. Schumm,¹³ A. Seiden,¹³
D. S. Chao,¹⁴ C. H. Cheng,¹⁴ B. Echenard,¹⁴ K. T. Flood,¹⁴ D. G. Hitlin,¹⁴ P. Ongmongkolkul,¹⁴
F. C. Porter,¹⁴ R. Andreassen,¹⁵ C. Fabby,¹⁵ Z. Huard,¹⁵ B. T. Meadows,¹⁵ M. D. Sokoloff,¹⁵ L. Sun,¹⁵
P. C. Bloom,¹⁶ W. T. Ford,¹⁶ A. Gaz,¹⁶ U. Nauenberg,¹⁶ J. G. Smith,¹⁶ S. R. Wagner,¹⁶ R. Ayad,^{17,*}
W. H. Toki,¹⁷ B. Spaan,¹⁸ K. R. Schubert,¹⁹ R. Schwierz,¹⁹ D. Bernard,²⁰ M. Verderi,²⁰ S. Playfer,²¹
D. Bettoni^{a,22} C. Bozzi^{a,22} R. Calabrese^{ab,22} G. Cibinetto^{ab,22} E. Fioravanti^{ab,22} I. Garzia^{ab,22} E. Luppi^{ab,22}
L. Piemontese^{a,22} V. Santoro^{a,22} R. Baldini-Ferrolli,²³ A. Calcaterra,²³ R. de Sangro,²³ G. Finocchiaro,²³
S. Martellotti,²³ P. Patteri,²³ I. M. Peruzzi,^{23,†} M. Piccolo,²³ M. Rama,²³ A. Zallo,²³ R. Contri^{ab,24} E. Guido^{ab,24}
M. Lo Vetere^{ab,24} M. R. Monge^{ab,24} S. Passaggio^{a,24} C. Patrignani^{ab,24} E. Robutti^{a,24} B. Bhuyan,²⁵ V. Prasad,²⁵
M. Morii,²⁶ A. Adametz,²⁷ U. Uwer,²⁷ H. M. Lacker,²⁸ P. D. Dauncey,²⁹ U. Mallik,³⁰ C. Chen,³¹ J. Cochran,³¹
W. T. Meyer,³¹ S. Prell,³¹ A. E. Rubin,³¹ A. V. Gritsan,³² N. Arnaud,³³ M. Davier,³³ D. Derkach,³³
G. Grosdidier,³³ F. Le Diberder,³³ A. M. Lutz,³³ B. Malaescu,³³ P. Roudeau,³³ A. Stocchi,³³ G. Wormser,³³
D. J. Lange,³⁴ D. M. Wright,³⁴ J. P. Coleman,³⁵ J. R. Fry,³⁵ E. Gabathuler,³⁵ D. E. Hutchcroft,³⁵ D. J. Payne,³⁵
C. Touramanis,³⁵ A. J. Bevan,³⁶ F. Di Lodovico,³⁶ R. Sacco,³⁶ G. Cowan,³⁷ J. Bougher,³⁸ D. N. Brown,³⁸
C. L. Davis,³⁸ A. G. Denig,³⁹ M. Fritsch,³⁹ W. Gradl,³⁹ K. Griessinger,³⁹ A. Hafner,³⁹ E. Prencipe,³⁹
R. J. Barlow,^{40,‡} G. D. Lafferty,⁴⁰ E. Behn,⁴¹ R. Cenci,⁴¹ B. Hamilton,⁴¹ A. Jawahery,⁴¹ D. A. Roberts,⁴¹
R. Cowan,⁴² D. Dujmic,⁴² G. Sciolla,⁴² R. Cheaib,⁴³ P. M. Patel,^{43,§} S. H. Robertson,⁴³ P. Biassoni^{ab,44}
N. Neri^{a,44} F. Palombo^{ab,44} L. Cremaldi,⁴⁵ R. Godang,^{45,¶} P. Sonnek,⁴⁵ D. J. Summers,⁴⁵ X. Nguyen,⁴⁶
M. Simard,⁴⁶ P. Taras,⁴⁶ G. De Nardo^{ab,47} D. Monorchio^{ab,47} G. Onorato^{ab,47} C. Sciacca^{ab,47} M. Martinelli,⁴⁸
G. Raven,⁴⁸ C. P. Jessop,⁴⁹ J. M. LoSecco,⁴⁹ K. Honscheid,⁵⁰ R. Kass,⁵⁰ J. Brau,⁵¹ R. Frey,⁵¹ N. B. Sinev,⁵¹
D. Strom,⁵¹ E. Torrence,⁵¹ E. Feltresi^{ab,52} M. Margoni^{ab,52} M. Morandin^{a,52} M. Posocco^{a,52} M. Rotondo^{a,52}
G. Simi^{a,52} F. Simonetto^{ab,52} R. Stroili^{ab,52} S. Akar,⁵³ E. Ben-Haim,⁵³ M. Bomben,⁵³ G. R. Bonneaud,⁵³
H. Briand,⁵³ G. Calderini,⁵³ J. Chauveau,⁵³ Ph. Leruste,⁵³ G. Marchiori,⁵³ J. Ocariz,⁵³ S. Sitt,⁵³ M. Biasini^{ab,54}
E. Manoni^{a,54} S. Pacetti^{ab,54} A. Rossi^{a,54} C. Angelini^{ab,55} G. Batignani^{ab,55} S. Bettarini^{ab,55} M. Carpinelli^{ab,55,**}
G. Casarosa^{ab,55} A. Cervelli^{ab,55} F. Forti^{ab,55} M. A. Giorgi^{ab,55} A. Lusiani^{ac,55} B. Oberhof^{ab,55} E. Paoloni^{ab,55}
A. Perez^{a,55} G. Rizzo^{ab,55} J. J. Walsh^{a,55} D. Lopes Pegna,⁵⁶ J. Olsen,⁵⁶ A. J. S. Smith,⁵⁶ R. Faccini^{ab,57}
F. Ferrarotto^{a,57} F. Ferroni^{ab,57} M. Gaspero^{ab,57} L. Li Gioi^{a,57} G. Piredda^{a,57} C. Büniger,⁵⁸ O. Grünberg,⁵⁸
T. Hartmann,⁵⁸ T. Leddig,⁵⁸ C. Voß,⁵⁸ R. Waldi,⁵⁸ T. Adye,⁵⁹ E. O. Olaiya,⁵⁹ F. F. Wilson,⁵⁹ S. Emery,⁶⁰
G. Hamel de Monchenault,⁶⁰ G. Vasseur,⁶⁰ Ch. Yèche,⁶⁰ F. Anulli^{a,61} D. Aston,⁶¹ D. J. Bard,⁶¹ J. F. Benitez,⁶¹
C. Cartaro,⁶¹ M. R. Convery,⁶¹ J. Dorfan,⁶¹ G. P. Dubois-Felsmann,⁶¹ W. Dunwoodie,⁶¹ M. Ebert,⁶¹ R. C. Field,⁶¹
B. G. Fulsom,⁶¹ A. M. Gabareen,⁶¹ M. T. Graham,⁶¹ C. Hast,⁶¹ W. R. Innes,⁶¹ P. Kim,⁶¹ M. L. Kocian,⁶¹
D. W. G. S. Leith,⁶¹ P. Lewis,⁶¹ D. Lindemann,⁶¹ B. Lindquist,⁶¹ S. Luitz,⁶¹ V. Luth,⁶¹ H. L. Lynch,⁶¹
D. B. MacFarlane,⁶¹ D. R. Muller,⁶¹ H. Neal,⁶¹ S. Nelson,⁶¹ M. Perl,⁶¹ T. Pulliam,⁶¹ B. N. Ratcliff,⁶¹
A. Roodman,⁶¹ A. A. Salnikov,⁶¹ R. H. Schindler,⁶¹ A. Snyder,⁶¹ D. Su,⁶¹ M. K. Sullivan,⁶¹ J. Va'vra,⁶¹
A. P. Wagner,⁶¹ W. F. Wang,⁶¹ W. J. Wisniewski,⁶¹ M. Wittgen,⁶¹ D. H. Wright,⁶¹ H. W. Wulsin,⁶¹ V. Ziegler,⁶¹

W. Park,⁶² M. V. Purohit,⁶² R. M. White,^{62,††} J. R. Wilson,⁶² A. Randle-Conde,⁶³ S. J. Sekula,⁶³ M. Bellis,⁶⁴ P. R. Burchat,⁶⁴ T. S. Miyashita,⁶⁴ E. M. T. Puccio,⁶⁴ M. S. Alam,⁶⁵ J. A. Ernst,⁶⁵ R. Gorodeisky,⁶⁶ N. Guttman,⁶⁶ D. R. Peimer,⁶⁶ A. Soffer,⁶⁶ S. M. Spanier,⁶⁷ J. L. Ritchie,⁶⁸ A. M. Ruland,⁶⁸ R. F. Schwitters,⁶⁸ B. C. Wray,⁶⁸ J. M. Izen,⁶⁹ X. C. Lou,⁶⁹ F. Bianchi^{ab,70} F. De Mori^{ab,70} A. Filippi^{a,70} D. Gamba^{ab,70} S. Zambito^{ab,70} L. Lanceri^{ab,71} L. Vitale^{ab,71} F. Martinez-Vidal,⁷² A. Oyanguren,⁷² P. Villanueva-Perez,⁷² H. Ahmed,⁷³ J. Albert,⁷³ Sw. Banerjee,⁷³ F. U. Bernlochner,⁷³ H. H. F. Choi,⁷³ G. J. King,⁷³ R. Kowalewski,⁷³ M. J. Lewczuk,⁷³ T. Lueck,⁷³ I. M. Nugent,⁷³ J. M. Roney,⁷³ R. J. Sobie,⁷³ N. Tasneem,⁷³ T. J. Gershon,⁷⁴ P. F. Harrison,⁷⁴ T. E. Latham,⁷⁴ H. R. Band,⁷⁵ S. Dasu,⁷⁵ Y. Pan,⁷⁵ R. Prepost,⁷⁵ and S. L. Wu⁷⁵

(The BABAR Collaboration)

¹Laboratoire d'Annecy-le-Vieux de Physique des Particules (LAPP),
Université de Savoie, CNRS/IN2P3, F-74941 Annecy-Le-Vieux, France

²Universitat de Barcelona, Facultat de Física, Departament ECM, E-08028 Barcelona, Spain

³INFN Sezione di Bari^a; Dipartimento di Fisica, Università di Bari^b, I-70126 Bari, Italy

⁴University of Bergen, Institute of Physics, N-5007 Bergen, Norway

⁵Lawrence Berkeley National Laboratory and University of California, Berkeley, California 94720, USA

⁶Ruhr Universität Bochum, Institut für Experimentalphysik 1, D-44780 Bochum, Germany

⁷University of British Columbia, Vancouver, British Columbia, Canada V6T 1Z1

⁸Brunel University, Uxbridge, Middlesex UB8 3PH, United Kingdom

⁹Budker Institute of Nuclear Physics SB RAS, Novosibirsk 630090^a,

Novosibirsk State University, Novosibirsk 630090^b,

Novosibirsk State Technical University, Novosibirsk 630092^c, Russia

¹⁰University of California at Irvine, Irvine, California 92697, USA

¹¹University of California at Riverside, Riverside, California 92521, USA

¹²University of California at Santa Barbara, Santa Barbara, California 93106, USA

¹³University of California at Santa Cruz, Institute for Particle Physics, Santa Cruz, California 95064, USA

¹⁴California Institute of Technology, Pasadena, California 91125, USA

¹⁵University of Cincinnati, Cincinnati, Ohio 45221, USA

¹⁶University of Colorado, Boulder, Colorado 80309, USA

¹⁷Colorado State University, Fort Collins, Colorado 80523, USA

¹⁸Technische Universität Dortmund, Fakultät Physik, D-44221 Dortmund, Germany

¹⁹Technische Universität Dresden, Institut für Kern- und Teilchenphysik, D-01062 Dresden, Germany

²⁰Laboratoire Leprince-Ringuet, Ecole Polytechnique, CNRS/IN2P3, F-91128 Palaiseau, France

²¹University of Edinburgh, Edinburgh EH9 3JZ, United Kingdom

²²INFN Sezione di Ferrara^a; Dipartimento di Fisica e Scienze della Terra, Università di Ferrara^b, I-44122 Ferrara, Italy

²³INFN Laboratori Nazionali di Frascati, I-00044 Frascati, Italy

²⁴INFN Sezione di Genova^a; Dipartimento di Fisica, Università di Genova^b, I-16146 Genova, Italy

²⁵Indian Institute of Technology Guwahati, Guwahati, Assam, 781 039, India

²⁶Harvard University, Cambridge, Massachusetts 02138, USA

²⁷Universität Heidelberg, Physikalisches Institut, D-69120 Heidelberg, Germany

²⁸Humboldt-Universität zu Berlin, Institut für Physik, D-12489 Berlin, Germany

²⁹Imperial College London, London, SW7 2AZ, United Kingdom

³⁰University of Iowa, Iowa City, Iowa 52242, USA

³¹Iowa State University, Ames, Iowa 50011-3160, USA

³²Johns Hopkins University, Baltimore, Maryland 21218, USA

³³Laboratoire de l'Accélérateur Linéaire, IN2P3/CNRS et Université Paris-Sud 11,
Centre Scientifique d'Orsay, F-91898 Orsay Cedex, France

³⁴Lawrence Livermore National Laboratory, Livermore, California 94550, USA

³⁵University of Liverpool, Liverpool L69 7ZE, United Kingdom

³⁶Queen Mary, University of London, London, E1 4NS, United Kingdom

³⁷University of London, Royal Holloway and Bedford New College, Egham, Surrey TW20 0EX, United Kingdom

³⁸University of Louisville, Louisville, Kentucky 40292, USA

³⁹Johannes Gutenberg-Universität Mainz, Institut für Kernphysik, D-55099 Mainz, Germany

⁴⁰University of Manchester, Manchester M13 9PL, United Kingdom

⁴¹University of Maryland, College Park, Maryland 20742, USA

⁴²Massachusetts Institute of Technology, Laboratory for Nuclear Science, Cambridge, Massachusetts 02139, USA

⁴³McGill University, Montréal, Québec, Canada H3A 2T8

⁴⁴INFN Sezione di Milano^a; Dipartimento di Fisica, Università di Milano^b, I-20133 Milano, Italy

⁴⁵University of Mississippi, University, Mississippi 38677, USA

⁴⁶Université de Montréal, Physique des Particules, Montréal, Québec, Canada H3C 3J7

⁴⁷INFN Sezione di Napoli^a; Dipartimento di Scienze Fisiche,
Università di Napoli Federico II^b, I-80126 Napoli, Italy

⁴⁸NIKHEF, National Institute for Nuclear Physics and High Energy Physics, NL-1009 DB Amsterdam, The Netherlands

⁴⁹University of Notre Dame, Notre Dame, Indiana 46556, USA

⁵⁰Ohio State University, Columbus, Ohio 43210, USA

⁵¹University of Oregon, Eugene, Oregon 97403, USA

⁵²INFN Sezione di Padova^a; Dipartimento di Fisica, Università di Padova^b, I-35131 Padova, Italy

⁵³Laboratoire de Physique Nucléaire et de Hautes Energies,

IN2P3/CNRS, Université Pierre et Marie Curie-Paris6,

Université Denis Diderot-Paris7, F-75252 Paris, France

⁵⁴INFN Sezione di Perugia^a; Dipartimento di Fisica, Università di Perugia^b, I-06123 Perugia, Italy

⁵⁵INFN Sezione di Pisa^a; Dipartimento di Fisica,

Università di Pisa^b; Scuola Normale Superiore di Pisa^c, I-56127 Pisa, Italy

⁵⁶Princeton University, Princeton, New Jersey 08544, USA

⁵⁷INFN Sezione di Roma^a; Dipartimento di Fisica,

Università di Roma La Sapienza^b, I-00185 Roma, Italy

⁵⁸Universität Rostock, D-18051 Rostock, Germany

⁵⁹Rutherford Appleton Laboratory, Chilton, Didcot, Oxon, OX11 0QX, United Kingdom

⁶⁰CEA, Irfu, SPP, Centre de Saclay, F-91191 Gif-sur-Yvette, France

⁶¹SLAC National Accelerator Laboratory, Stanford, California 94309 USA

⁶²University of South Carolina, Columbia, South Carolina 29208, USA

⁶³Southern Methodist University, Dallas, Texas 75275, USA

⁶⁴Stanford University, Stanford, California 94305-4060, USA

⁶⁵State University of New York, Albany, New York 12222, USA

⁶⁶Tel Aviv University, School of Physics and Astronomy, Tel Aviv, 69978, Israel

⁶⁷University of Tennessee, Knoxville, Tennessee 37996, USA

⁶⁸University of Texas at Austin, Austin, Texas 78712, USA

⁶⁹University of Texas at Dallas, Richardson, Texas 75083, USA

⁷⁰INFN Sezione di Torino^a; Dipartimento di Fisica Sperimentale, Università di Torino^b, I-10125 Torino, Italy

⁷¹INFN Sezione di Trieste^a; Dipartimento di Fisica, Università di Trieste^b, I-34127 Trieste, Italy

⁷²IFIC, Universitat de Valencia-CSIC, E-46071 Valencia, Spain

⁷³University of Victoria, Victoria, British Columbia, Canada V8W 3P6

⁷⁴Department of Physics, University of Warwick, Coventry CV4 7AL, United Kingdom

⁷⁵University of Wisconsin, Madison, Wisconsin 53706, USA

We measure the mass difference, Δm_0 , between the $D^*(2010)^+$ and the D^0 and the natural line width, Γ , of the transition $D^*(2010)^+ \rightarrow D^0\pi^+$. The data were recorded with the BABAR detector at center-of-mass energies at and near the $\Upsilon(4S)$ resonance, and correspond to an integrated luminosity of approximately 477 fb^{-1} . The D^0 is reconstructed in the decay modes $D^0 \rightarrow K^-\pi^+$ and $D^0 \rightarrow K^-\pi^+\pi^-\pi^+$. For the decay mode $D^0 \rightarrow K^-\pi^+$ we obtain $\Gamma = (83.4 \pm 1.7 \pm 1.5) \text{ keV}$ and $\Delta m_0 = (145\,425.6 \pm 0.6 \pm 1.8) \text{ keV}$, where the quoted errors are statistical and systematic, respectively. For the $D^0 \rightarrow K^-\pi^+\pi^-\pi^+$ mode we obtain $\Gamma = (83.2 \pm 1.5 \pm 2.6) \text{ keV}$ and $\Delta m_0 = (145\,426.6 \pm 0.5 \pm 2.0) \text{ keV}$. The combined measurements yield $\Gamma = (83.3 \pm 1.2 \pm 1.4) \text{ keV}$ and $\Delta m_0 = (145\,425.9 \pm 0.4 \pm 1.7) \text{ keV}$; the width is a factor of approximately 12 times more precise than the previous value, while the mass difference is a factor of approximately 6 times more precise.

PACS numbers: 13.20.Fc, 13.25.Ft, 14.40.Lb, 12.38.Gc, 12.38.Qk, 12.39.Ki, 12.39.Pn

The line width of the $D^*(2010)^+$ (D^{*+}) provides a window into a nonperturbative regime of strong interaction physics where the charm quark is the heavier meson constituent [1–3]. The line width provides an experimental test of D meson spectroscopic models, and is related to the strong coupling of the $D^*D\pi$ system, $g_{D^*D\pi}$. In the heavy-quark limit, which is not necessarily a good approximation for the charm quark [4], this coupling can be related to the universal coupling of heavy mesons to a pion, \hat{g} . Since the decay $B^* \rightarrow B\pi$ is kinematically forbidden, it is not possible to measure the coupling $g_{B^*B\pi}$ directly. However, the D and B systems can be related through \hat{g} , allowing the calculation of $g_{B^*B\pi}$, which is needed for a model-independent extraction of $|V_{ub}|$ [5, 6] and which forms one of the larger theoretical uncertain-

ties for the determination of $|V_{ub}|$ [7].

We study the $D^{*+} \rightarrow D^0\pi^+$ transition, using the $D^0 \rightarrow K^-\pi^+$ and $D^0 \rightarrow K^-\pi^+\pi^-\pi^+$ decay modes, to extract values of the D^{*+} width Γ and the difference between the D^{*+} and D^0 masses Δm_0 . Values are reported in natural units and the use of charge conjugate reactions is implied throughout this paper. The only prior measurement of the width is $\Gamma = (96 \pm 4 \pm 22) \text{ keV}$ by the CLEO collaboration, where the uncertainties are statistical and systematic, respectively [8]. In the present analysis, we use a data sample that is approximately 50 times larger. This allows us to apply restrictive selection criteria to reduce background and to investigate sources of systematic uncertainty with high precision.

To extract Γ , we fit the distribution of the mass differ-

ence between the reconstructed D^{*+} and the D^0 masses, Δm . The signal component is described with a P-wave relativistic Breit-Wigner (RBW) function convolved with a resolution function based on a Geant4 Monte Carlo (MC) simulation of the detector response [9].

The full width at half maximum (FWHM) of the RBW line shape (≈ 100 keV) is much less than the FWHM of the almost Gaussian resolution function which describes more than 99% of the signal (≈ 300 keV). Therefore, near the peak, the observed FWHM is dominated by the resolution function shape. However, the shapes of the resolution function and the RBW differ far away from the pole position. Starting ($1.5 - 2.0$) MeV from the pole position, and continuing to ($5 - 10$) MeV away (depending on the D^0 decay channel), the RBW tails are much larger. The observed event rates in this region are strongly dominated by the intrinsic line width of the signal, not the signal resolution function or the background rate. We use the very different resolution and RBW shapes, combined with the good signal-to-background rate far from the peak, to measure Γ precisely [10].

This analysis is based on a data set corresponding to an integrated luminosity of approximately 477 fb^{-1} recorded at, and 40 MeV below, the $\Upsilon(4S)$ resonance [11]. The data were collected with the *BABAR* detector at the PEP-II asymmetric energy e^+e^- collider, located at the SLAC National Accelerator Laboratory. The *BABAR* detector is described in detail elsewhere [12, 13]; we summarize the relevant features below. The momenta of charged particles are measured with a combination of a cylindrical drift chamber (DCH) and a 5-layer silicon vertex tracker (SVT), both operating within the 1.5 T magnetic field of a superconducting solenoid. Information from a ring-imaging Cherenkov detector is combined with specific ionization (dE/dx) measurements from the SVT and DCH to identify charged kaon and pion candidates. Electrons are identified, and photons measured, with a CsI(Tl) electromagnetic calorimeter. The return yoke of the superconducting coil is instrumented with tracking chambers for the identification of muons.

We remove a large amount of combinatorial and B meson decay background by requiring D^{*+} mesons produced in $e^+e^- \rightarrow c\bar{c}$ reactions to exhibit an e^+e^- center-of-mass-frame momentum greater than 3.6 GeV. The entire decay chain is fit using a kinematic fitter with geometric constraints at the production and decay vertex of the D^0 and the additional constraint that the D^{*+} laboratory momentum points back to the luminous region of the event. The pion from D^{*+} decay is referred to as the ‘‘slow pion’’ (denoted π_s^+) because of the limited phase space available in the D^{*+} decay. The selection criteria are chosen to provide a large signal-to-background ratio (S/B), in order to increase the sensitivity to the long signal (RBW) tails in the Δm distribution; they are not optimized for statistical significance. The criteria are briefly mentioned here and presented in detail in the

archival reference for this analysis [10]. The resolution in Δm is dominated by the resolution of the π_s^+ momentum, especially the uncertainty of its direction due to Coulomb multiple scattering. We implement criteria to select well-measured pions. We define our acceptance angle to exclude the very-forward region of the detector, where track momenta are not accurately reconstructed, as determined using an independent sample of reconstructed $K_S^0 \rightarrow \pi^-\pi^+$ decays. The K_S^0 reconstructed mass is observed to vary as a function of the polar angle θ of the K_S^0 momentum measured in the laboratory frame with respect to the electron beam axis. To remove contributions from the very-forward region of the detector we reject events with any D^{*+} daughter track for which $\cos\theta > 0.89$; this criterion reduces the final samples by approximately 10%.

Our fitting procedure involves two steps. In the first step we model the finite detector resolution associated with track reconstruction by fitting the Δm distribution for correctly reconstructed MC events using a sum of three Gaussians and a function to describe the non-Gaussian component [10]. These simulated D^{*+} decays are generated with $\Gamma = 0.1$ keV, so that the observed spread of the MC distribution can be attributed to event reconstruction. The non-Gaussian function describes π_s^+ decays in flight to a μ , for which coordinates from both the π and μ segments are used in track reconstruction.

The second step uses the resolution shape parameters from the first step and convolves the Gaussian components with a RBW function to fit the measured Δm distribution in data. The RBW function is defined by

$$\frac{d\Gamma(m)}{dm} = \frac{m\Gamma_{D^*D\pi}(m) m_0\Gamma}{(m_0^2 - m^2)^2 + (m_0\Gamma_{\text{Total}}(m))^2}, \quad (1)$$

where $\Gamma_{D^*D\pi}$ is the partial width to $D^0\pi_s^+$, m is the $D^0\pi_s^+$ invariant mass, m_0 is the invariant mass at the pole, $\Gamma_{\text{Total}}(m)$ is the total D^{*+} decay width, and Γ is the natural line width we wish to measure. The partial width is defined by

$$\Gamma_{D^*D\pi}(m) = \Gamma \left(\frac{\mathcal{F}_{D\pi}^\ell(p_0)}{\mathcal{F}_{D\pi}^\ell(p)} \right)^2 \left(\frac{p}{p_0} \right)^{2\ell+1} \left(\frac{m_0}{m} \right). \quad (2)$$

Here $\ell = 1$, $\mathcal{F}_{D\pi}^{\ell=1}(p) = \sqrt{1+r^2p^2}$ is a Blatt-Weisskopf form factor for a vector particle with radius parameter r and daughter momentum p , and the subscript zero denotes a quantity measured at the mass pole m_0 [14, 15]. We use the value $r = 1.6 \text{ GeV}^{-1}$ from Ref. [16]. For the purpose of fitting the Δm distribution, we obtain $d\Gamma(\Delta m)/d\Delta m$ from Eqs. (1) and (2) through the substitution $m = m(D^0) + \Delta m$, where $m(D^0)$ is the nominal D^0 mass [17].

As in the CLEO analysis [8], we approximate the total D^{*+} decay width $\Gamma_{\text{Total}}(m) \approx \Gamma_{D^*D\pi}(m)$, ignoring the electromagnetic contribution from $D^{*+} \rightarrow D^+\gamma$. This

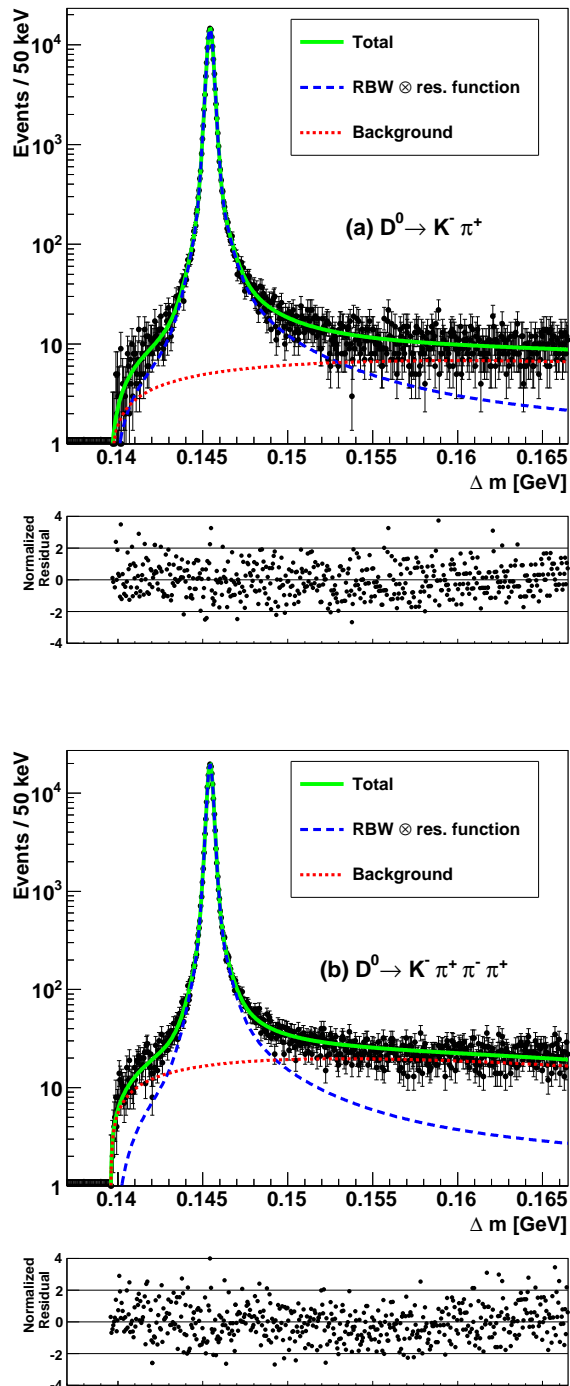


FIG. 1. (color online) Fits to data for the $D^0 \rightarrow K^- \pi^+$ and $D^0 \rightarrow K^- \pi^+ \pi^- \pi^+$ decay modes. The total probability density function (PDF) is shown as the solid curve, the convolved RBW-Gaussian signal as the dashed curve, and the background as the dotted curve. The total PDF and signal component are indistinguishable in the peak region. Normalized residuals are defined as $(N_{\text{observed}} - N_{\text{predicted}}) / \sqrt{N_{\text{predicted}}}$.

approximation has a negligible effect on the extracted values, as it appears only in the denominator of the RBW function.

To allow for differences between MC simulation and data, the root-mean-square deviation of each Gaussian component of the resolution function is allowed to scale in the fit process by the common factor $(1 + \epsilon)$. Events that contribute to the non-Gaussian component have a well-understood origin (π_s decay in flight), which is accurately reproduced by MC simulation. In the fit to data, the non-Gaussian function has a fixed shape and relative fraction, and is not convolved with the RBW. The relative contribution of the non-Gaussian function is small ($\lesssim 0.5\%$ of the signal), and the results from fits to validation signal-MC samples are unbiased without convolving this term. The background is described by a phase-space model of continuum background near the kinematic threshold [10]. We fit the Δm distribution from the kinematic threshold to $\Delta m = 0.1665$ GeV using a binned maximum likelihood fit and an interval width of 50 keV.

In the initial fits to data, we observed a strong dependence of Δm_0 on the slow pion momentum. This dependence, which originates in the modeling of the magnetic field map and the material in the beam pipe and SVT, is not replicated in the simulation. Previous *BABAR* analyses have observed similar effects, for example the measurement of the Λ_c^+ mass [18]. In that analysis the material model of the SVT was altered in an attempt to correct for the energy loss and the under-represented small-angle multiple scattering (due to nuclear Coulomb scattering). However, the momentum dependence of the reconstructed Λ_c^+ mass could be removed only by adding an unphysical amount of material to the SVT. In this analysis we use a different approach to correct the observed momentum dependence and adjust track momenta after reconstruction.

We use a sample of $K_S^0 \rightarrow \pi^+ \pi^-$ events from $D^{*+} \rightarrow D^0 \pi_s^+$ decays, where $D^0 \rightarrow K_S^0 \pi^+ \pi^-$, and require that the K_S^0 daughter pions satisfy the same tracking criteria as the π_s^+ candidates for the $D^0 \rightarrow K^- \pi^+$ and $D^0 \rightarrow K^- \pi^+ \pi^- \pi^+$ signal modes. The K_S^0 decay vertex is required to lie inside the beam pipe and to be well separated from the D^0 vertex. These selection criteria yield an extremely clean K_S^0 sample (over 99.5% pure), which is used to determine three fractional corrections to the overall magnetic field and to the energy losses in the beam pipe and, separately, in the SVT. We determine the best set of correction parameters by minimizing the difference between the $\pi^+ \pi^-$ invariant mass and the current world average for the K^0 mass (497.614 ± 0.024 MeV) [17] in 20 intervals of laboratory momentum in the range 0.0 to 2.0 GeV. The best-fit parameters increase the magnitude of the magnetic field by 4.5 Gauss and increase the energy loss in the beam pipe and SVT by 1.8% and 5.9%, respectively [10]. The momentum-dependence of Δm_0 in the preliminary results was mostly due to the slow pion.

However, the correction is applied to all D^{*+} daughter tracks. All fits to data described in this analysis are performed using masses and Δm values calculated using corrected momenta. Simulated events do not require correction because the same field and material models used to propagate tracks are used for their reconstruction.

Figure 1 presents the results of the fits to data for both the $D^0 \rightarrow K^- \pi^+$ and $D^0 \rightarrow K^- \pi^+ \pi^- \pi^+$ decay modes. The normalized residuals show good agreement between the data and our fits. Table I summarizes the results of the fits to data for both D^0 decay modes. The table also shows S/B at the peak and in the high Δm tail of each distribution.

TABLE I. Summary of the results from the fits to data for the $D^0 \rightarrow K^- \pi^+$ and $D^0 \rightarrow K^- \pi^+ \pi^- \pi^+$ channels (statistical uncertainties only). S/B is the ratio of the convolved signal PDF to the background PDF at the given Δm and ν is the number of degrees of freedom.

Parameter	$D^0 \rightarrow K\pi$	$D^0 \rightarrow K\pi\pi\pi$
Number of signal events	138 536 \pm 383	174 297 \pm 434
Γ (keV)	83.3 \pm 1.7	83.2 \pm 1.5
scale factor, $(1 + \epsilon)$	1.06 \pm 0.01	1.08 \pm 0.01
Δm_0 (keV)	145 425.6 \pm 0.6	145 426.6 \pm 0.5
S/B at peak ($\Delta m = 0.14542$ (GeV))	2700	1130
S/B at tail ($\Delta m = 0.1554$ (GeV))	0.8	0.3
χ^2/ν	574/535	556/535

We estimate systematic uncertainties related to a variety of sources. The data are divided into disjoint subsets corresponding to intervals of D^{*+} laboratory momentum, D^{*+} laboratory azimuthal angle ϕ , and reconstructed D^0 mass, in order to search for variations larger than those expected from statistical fluctuations. These are evaluated using a method similar to the PDG scale factor [10, 17]. The corrections to the overall momentum scale and dE/dx loss in detector material are varied to account for the uncertainty on the K_S^0 mass. To estimate the uncertainty in the Blatt-Weisskopf radius we model the D^{*+} as a point-like particle. We vary the parameters of the resolution function according to the covariance matrix reported by the fit to estimate systematic uncertainty of the resolution shape. We vary the end point used in the fit, which affects whether events are assigned to the signal or background component. This variation allows us to evaluate a systematic uncertainty associated with the background parametrization; within this systematic uncertainty, the residual plots shown in Fig. 1 are consistent with being entirely flat. Additionally, we vary the description of the background distribution near threshold. We fit MC validation samples to estimate systematic uncertainties associated with possible biases. Finally, we

use additional MC validation studies to estimate possible systematic uncertainties due to radiative effects. All these uncertainties are estimated independently for the $D^0 \rightarrow K^- \pi^+$ and $D^0 \rightarrow K^- \pi^+ \pi^- \pi^+$ modes, as discussed in detail in Ref. [10] and summarized in Table II.

The largest systematic uncertainty arises from an observed sinusoidal dependence for Δm_0 on ϕ . Variations with the same signs and phases are seen for the reconstructed D^0 mass in both $D^0 \rightarrow K^- \pi^+$, $D^0 \rightarrow K^- \pi^+ \pi^- \pi^+$, and for the K_S^0 mass. An extended investigation revealed that at least part of this dependence originates from small errors in the magnetic field from the map used in track reconstruction [10]. The important aspect for this analysis is that the average value is unbiased by the variation in ϕ , which we verified using the reconstructed K_S^0 mass value. The width does not display a ϕ dependence, but each mode is assigned a small uncertainty because some deviations from uniformity are observed. The lack of a systematic variation of Γ with respect to ϕ is notable because Δm_0 shows a clear dependence such that the results from the $D^0 \rightarrow K^- \pi^+$ and $D^0 \rightarrow K^- \pi^+ \pi^- \pi^+$ samples are highly correlated and shift together. We fit the Δm_0 values with a sinusoidal function and take half of the amplitude as the estimate of the uncertainty.

The results for the two independent D^0 decay modes agree within their uncertainties. The dominant systematic uncertainty on the RBW pole position comes from the variation in ϕ (1.5 – 1.9 keV). For the decay mode $D^0 \rightarrow K^- \pi^+$ we find $\Gamma = (83.4 \pm 1.7 \pm 1.5)$ keV and $\Delta m_0 = (145 425.6 \pm 0.6 \pm 1.8)$ keV, while for the decay mode $D^0 \rightarrow K^- \pi^+ \pi^- \pi^+$ we find $\Gamma = (83.2 \pm 1.5 \pm 2.6)$ keV and $\Delta m_0 = (145 426.6 \pm 0.5 \pm 2.0)$ keV. Accounting for correlations, we obtain the combined measurement values $\Gamma = (83.3 \pm 1.2 \pm 1.4)$ keV and $\Delta m_0 = (145 425.9 \pm 0.4 \pm 1.7)$ keV.

Using the relationship between the width and the coupling constant [10], we can determine the experimental value of $g_{D^{*+}D^0\pi^+}$. Using Γ and the masses from Ref. [17] we determine the experimental coupling $g_{D^{*+}D^0\pi^+}^{\text{exp}} = 16.92 \pm 0.13 \pm 0.14$, where we have ignored the electromagnetic contribution from $D^{*+} \rightarrow D^+ \gamma$. The universal coupling is directly related to $g_{D^*D\pi}$ by $\hat{g} = g_{D^{*+}D^0\pi^+} f_\pi / (2\sqrt{m_{D^0} m_{D^{*+}}})$. This parametrization is different from that used by CLEO [8]; it is chosen to match a common convention in the context of chiral perturbation theory, as in Refs. [4, 19]. With this relation and $f_\pi = 130.41$ MeV, we find $\hat{g}^{\text{exp}} = 0.570 \pm 0.004 \pm 0.005$.

Di Piero and Eichten [20] present results in terms of R , the ratio of the width of a given state to the universal coupling constant. At the time of their publication, $\hat{g} = 0.82 \pm 0.09$ was consistent with the values from all of the modes in Ref. [20]. In 2010, *BABAR* published much more precise mass and width results for the $D_1(2460)^0$

TABLE II. Summary of systematic uncertainties with correlation ρ between the $D^0 \rightarrow K^- \pi^+$ and $D^0 \rightarrow K^- \pi^+ \pi^- \pi^+$ modes. The $K^- \pi^+$ and $K^- \pi^+ \pi^- \pi^+$ invariant masses are denoted by $m(D_{\text{reco}}^0)$.

Source	$\sigma_{sys}(\Gamma)$ [keV]		ρ	$\sigma_{sys}(\Delta m_0)$ [keV]		ρ
	$K\pi$	$K\pi\pi\pi$		$K\pi$	$K\pi\pi\pi$	
Disjoint D^{*+} momentum variation	0.88	0.98	0.47	0.16	0.11	0.28
Disjoint $m(D_{\text{reco}}^0)$ variation	0.00	1.53	0.56	0.00	0.00	0.22
Disjoint azimuthal variation	0.62	0.92	-0.04	1.50	1.68	0.84
Magnetic field and material model	0.29	0.18	0.98	0.75	0.81	0.99
Blatt-Weisskopf radius	0.04	0.04	0.99	0.00	0.00	1.00
Variation of resolution shape parameters	0.41	0.37	0.00	0.17	0.16	0.00
Δm fit range	0.83	0.38	-0.42	0.08	0.04	0.35
Background shape near threshold	0.10	0.33	1.00	0.00	0.00	0.00
Interval width for fit	0.00	0.05	0.99	0.00	0.00	0.00
Bias from validation	0.00	1.50	0.00	0.00	0.00	0.00
Radiative effects	0.25	0.11	0.00	0.00	0.00	0.00
Total	1.5	2.6		1.7	1.9	

TABLE III. Updated coupling constant values using the latest width measurements. Ratios are taken from Ref. [20].

State	Width (Γ)	$R = \Gamma/\hat{g}^2$ (model)	\hat{g}
$D^*(2010)^+$	$83.3 \pm 1.3 \pm 1.4$ keV	143 keV	0.76 ± 0.01
$D_1(2420)^0$	$31.4 \pm 0.5 \pm 1.3$ MeV	16 MeV	1.40 ± 0.03
$D_2^*(2460)^0$	$50.5 \pm 0.6 \pm 0.7$ MeV	38 MeV	1.15 ± 0.01

and $D_2^*(2460)^0$ mesons [21]. Using these values, our measurement of Γ , and the ratios from Ref. [20], we calculate new values for the coupling constant \hat{g} . Table III shows the updated results. We estimate the uncertainty on \hat{g} assuming $\sigma_\Gamma \ll \Gamma$. The updated widths reveal significant differences among the extracted values of \hat{g} . The order of magnitude increase in precision of the D^{*+} width measurement compared to previous studies confirms the observed inconsistency between the measured D^{*+} width and the chiral quark model calculation by Di Pierro and Eichten [20].

After completing this analysis, we became aware of Rosner's 1985 prediction that the D^{*+} natural line width should be 83.9 keV [22]. He calculated this assuming a single quark transition model to use P-wave $K^* \rightarrow K\pi$ decays to predict P-wave $D^* \rightarrow D\pi$ decay properties. Although he did not report an error estimate for this calculation in that work, his central value falls well within our experimental precision. Using the same procedure and current measurements, the prediction becomes (80.5 ± 0.1) keV [23]. A new lattice gauge calculation yielding $\Gamma(D^{*+}) = (76 \pm 7_{-10}^{+8})$ keV, has also been reported recently [1].

We are grateful for the excellent luminosity and machine conditions provided by our PEP-II colleagues, and for the substantial dedicated effort from the comput-

ing organizations that support BABAR. The collaborating institutions wish to thank SLAC for its support and kind hospitality. This work is supported by DOE and NSF (USA), NSERC (Canada), CEA and CNRS-IN2P3 (France), BMBF and DFG (Germany), INFN (Italy), FOM (The Netherlands), NFR (Norway), MES (Russia), MINECO (Spain), STFC (United Kingdom). Individuals have received support from the Marie Curie EIF (European Union) and the A. P. Sloan Foundation (USA). The University of Cincinnati is gratefully acknowledged for its support of this research through a WISE (Women in Science and Engineering) fellowship to C. Fabby.

* Now at the University of Tabuk, Tabuk 71491, Saudi Arabia

† Also with Università di Perugia, Dipartimento di Fisica, Perugia, Italy

‡ Now at the University of Huddersfield, Huddersfield HD1 3DH, UK

§ Deceased

¶ Now at University of South Alabama, Mobile, Alabama 36688, USA

** Also with Università di Sassari, Sassari, Italy

†† Now at Universidad Técnica Federico Santa María, Valparaíso, Chile 2390123

- [1] D. Becirevic and F. Sanfilippo, Phys. Lett. B **721**, 94 (2013).
- [2] P. Singer, Acta Phys. Pol. B **30**, 3849 (1999).
- [3] D. Guetta and P. Singer, Nucl. Phys. Proc. Suppl. **93**, 134 (2001).
- [4] B. El-Bennich, M. A. Ivanov, and C. D. Roberts, Phys. Rev. C **83**, 025205 (2011).
- [5] G. Burdman *et al.*, Phys. Rev. D **49**, 2331 (1994).
- [6] C. Arnesen *et al.*, Phys. Rev. Lett. **95**, 071802 (2005).
- [7] J. Bailey *et al.*, Phys. Rev. D **79**, 054507 (2009).
- [8] A. Anastassov *et al.* (CLEO Collaboration), Phys. Rev. D **65**, 032003 (2002).

- [9] S. Agostinelli *et al.* (Geant4 Collaboration), Nucl. Instr. Methods Phys. Res., Sect. A **506**, 250 (2003).
- [10] J. P. Lees *et al.* (BABAR Collaboration), Submitted to Phys. Rev. D (2013), arXiv:1304.5009 [hep-ex].
- [11] J. P. Lees *et al.* (BABAR Collaboration), Nucl. Instr. Methods Phys. Res., Sect. A **726**, 203 (2013).
- [12] B. Aubert *et al.* (BABAR Collaboration), Nucl. Instr. Methods Phys. Res., Sect. A **479**, 1 (2002).
- [13] B. Aubert *et al.* (BABAR Collaboration), in press in Nucl. Instr. Methods Phys. Res., Sect. A., arXiv:1305.3560 (2013).
- [14] J. M. Blatt and V. F. Weisskopf, *Theoretical Nuclear Physics* (John Wiley & Sons, New York, 1952).
- [15] F. von Hippel and C. Quigg, Phys. Rev. D **5**, 624 (1972).
- [16] A. J. Schwartz (for the E791 Collaboration), Contribution to the 5th International Conference on Quark Confinement and the Hadron Spectrum, Gargnano, Italy, September 10-14, 2002, arXiv:hep-ex/0212057.
- [17] J. Beringer *et al.* (Particle Data Group), Phys. Rev. D **86**, 010001 (2012).
- [18] B. Aubert *et al.* (BABAR Collaboration), Phys. Rev. D **72**, 052006 (2005).
- [19] A. Abada *et al.*, Phys. Rev. D **66**, 074504 (2002).
- [20] M. Di Pierro and E. Eichten, Phys. Rev. D **64**, 114004 (2001).
- [21] P. del Amo Sanchez *et al.* (BABAR Collaboration), Phys. Rev. D **82**, 111101(R) (2010).
- [22] J. L. Rosner, Comments Nucl. Part. Phys. **16**, 109 (1986).
- [23] J. L. Rosner, (private communication), arXiv:1307.2550.